Available online at www.sciencedirect.com
ScienceDirect
Journal of Sound and Vibration 306 (2007) 297–317
JOURNAL OF SOUND AND VIBRATION
www.elsevier.com/locate/jsvi

A reduced order model for optimal design of 2-mdof adjacent structures connected by hysteretic dampers

M. Basili*, M. De Angelis

Department of Structural and Geotechnical Engineering, University of Rome, 'La Sapienza', Via Eudossiana 18, 00184, Rome, Italy

Received 12 October 2006; received in revised form 3 May 2007; accepted 3 May 2007
Available online 28 June 2007

Abstract

Coupling adjacent structures with supplemental control devices appears to be a useful method to mitigate structural response. In this work, a reduced order model for optimal design of two multi-degree-of-freedom (2-mdof) structures connected by hysteretic dampers is studied. The seismic input is modeled as a Gaussian white-noise stationary stochastic process. Since the passive connection is modeled as a nonlinear hysteretic element, represented by the differential Bouc–Wen law, a stochastic linearization technique is applied in order to simplify the problem. The design procedure is based on replacing the 2-mdof system, with a generalized two single-degree-of-freedom (2-sdof) system, by using the principle of virtual displacements; here, each structure is represented by an elementary oscillator interconnected by a hysteretic device. Once the equivalent structural parameters of the generalized 2-sdof system is known, it is possible to carry out the optimal design of the connection by using simple spectra obtained by the authors in a previous work, where the optimal design of a horizontal hysteretic link connecting a 2-sdof system has been studied and solved. Illustrative examples confirm the entire methodology and also verify the effectiveness of hysteretic connection on seismic response.

1. Introduction

Interconnecting two adjacent structures with special devices which are passively, semi-actively or actively controlled, represents a valid approach for preventing damage due to general dynamic inputs. Such applications can be found in many fields, from aerospace, to mechanical, industrial, and civil engineering. A good way to improve response reduction in the system is to create properly located special links for enhancing damping, stiffness, or strength [1]. The simplest as well as most effective devices applicable to this objective appear to be based on passive energy dissipation [2]. The mechanical behavior of passive devices may be linear and nonlinear: the linear behavior is typically modeled as Voigt or Maxwell model, while the nonlinear behavior is generally modeled as Bouc–Wen model [3].

The optimal design of linear passive connection (PC) devices coupling two adjacent single-degree-of-freedom (sdof) [4,5] and multi-degree-of-freedom (mdof) systems [6] is treated in literature. In particular, the paper by Aida et al. [7] proposes: in order to increase the structural damping performance, a simple procedure

*Corresponding author. Tel.: +39 06 44585399.
E-mail address: michela.basili@uniroma1.it (M. Basili).

0022-460X/$ - see front matter © 2007 Elsevier Ltd. All rights reserved.
doi:10.1016/j.jsv.2007.05.012

should be administered that entails interconnecting two adjacent mdof structures with a member consisting of a spring and a damper (Voigt model). By using only the first vibration mode of each structure in the modal dynamic equations, the resulting equations of motion correspond to those of an equivalent 2-sdof system, and the optimum parameters of the connection are calculated by using a tuning method. This procedure furnishes synthetic indications about the optimal values of spring and damping coefficients, and yields a simple relation between the optimal design of 2-mdof and 2-sdof model of adjacent structures.

The analogous problem regarding optimal design of two adjacent structures interconnected by nonlinear hysteretic devices has also been treated in literature [8–12]. In this case, simple and general information about the optimal design of nonlinear connecting hysteretic devices is given, though only for two adjacent sdof structures [9]. Whereas, for 2-mdof systems, only a small amount of synthetic and general information about number and position of devices is evidenced.

This paper thus aims to give a simple methodology to perform an optimal design for nonlinear hysteretic devices interconnecting two adjacent structures described by a 2-mdof system excited by seismic input, where the input is modeled as a Gaussian white-noise stationary stochastic process. As the entire system is nonlinear, a stochastic linearization technique is applied in order to simplify the problem. Since the optimal design of such devices generally implies that a large number of equations must be solved iteratively, a procedure based on a simplified structural model is thus proposed within this paper. The 2-mdof system connected by nonlinear hysteretic devices, is replaced with a reduced order model represented by a generalized 2-sdof system. Here each structure is represented by an elementary oscillator interconnected by a hysteretic device through the principle of virtual displacements [13]. Once the equivalent structural parameters of the generalized 2-sdof system are known, the optimal design is carried out through simple spectra obtained by the authors in a previous work [9]: here, the optimal design of horizontal hysteretic links connecting a 2-sdof system has been studied and solved. Finally, the proposed methodology and the effectiveness of hysteretic connection on seismic response are evaluated performing the analysis on the 2-mdof system through three different illustrative numerical examples.

2. Problem definition

2.1. Equations of motion for 2-mdof systems

The structural problem of interconnecting 2-mdof plane structures (Fig. 1), having N_1 and N_2 degrees of freedom ($N_1 \geqslant N_2$), by N_u horizontal hysteretic passive devices ($N_u \leqslant N_2$), can be expressed by the following

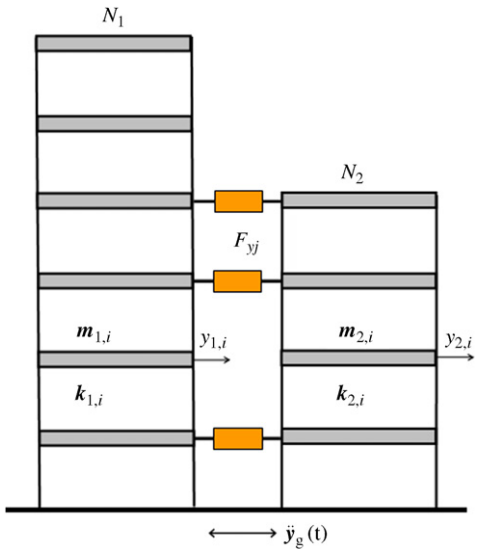

Fig. 1. The 2-mdof structural model.

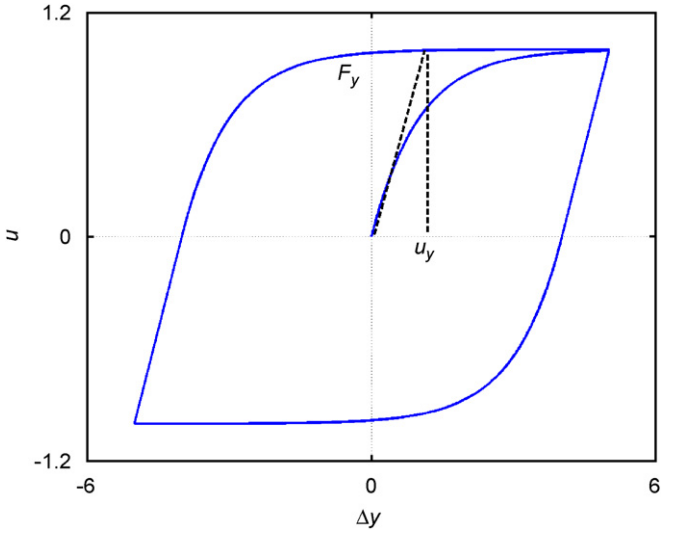

Fig. 2. u-Δy graph for $\bar{A} = 1$, $\bar{\beta} = 0.5$, $\bar{\gamma} = 0.5$, $n = 1$.

system representing the equations of motion:

$$\begin{cases} \mathbf{M}_1\ddot{\mathbf{Y}}_1(t) + \mathbf{C}_1\dot{\mathbf{Y}}_1(t) + \mathbf{K}_1\mathbf{Y}_1(t) = \mathbf{B}_{u1}^{\mathrm{T}}\mathbf{u}(t) - \mathbf{M}_1\boldsymbol{\tau}_1\ddot{y}_g(t), \\ \mathbf{M}_2\ddot{\mathbf{Y}}_2(t) + \mathbf{C}_2\dot{\mathbf{Y}}_2(t) + \mathbf{K}_2\mathbf{Y}_2(t) = -\mathbf{B}_{u2}^{\mathrm{T}}\mathbf{u}(t) - \mathbf{M}_2\boldsymbol{\tau}_2\ddot{y}_g(t), \end{cases} \tag{1}$$

where $(i = 1, 2)$: $\mathbf{M}_i$, $\mathbf{C}_i$, and $\mathbf{K}_i$ are, respectively, the $N_i \times N_i$ dimensional mass, damping and stiffness matrices; $\mathbf{Y}_i$ is the N_i dimensional lateral displacement vector; $\mathbf{u}(t)$ the N_u dimensional device force vector and $\mathbf{B}_{ui}$ the $N_u \times N_i$ dimensional allocation matrix; finally, $\ddot{y}_g(t)$ the ground acceleration, (which represents the seismic excitation), while $\boldsymbol{\tau}_i$ is the N_i dimensional unit vector.

The PC is modeled as a nonlinear hysteretic element [3]; the jth device, with zero post-yield stiffness, has the following constitutive law:

$$u_j(t) = F_{yj} z_j(t) \quad j = 1, 2, \ldots, \mathrm{N}_u, \tag{2}$$

where F_{yj} is a force parameter and z_j is the auxiliary argument, expressed in nondimensional form, and defined by the Bouc–Wen model through the nonlinear first-order differential equation:

$$\dot{z}_j = -\bar{g}_j(z_j, \Delta\dot{y}_j)\Delta\dot{y}_j / u_{yj}, \tag{3}$$

with

$$\bar{g}_j(z_j, (\Delta\dot{y}_j)) = -\bar{\gamma}_j \operatorname{sgn}(z_j, (\Delta\dot{y}_j)) z_j |z_j|^{n_j - 1} - \bar{\beta}_j |z_j|^{n_j} + \bar{A}_j, \tag{4}$$

where $\Delta\dot{y}_j = \dot{y}_{2j} - \dot{y}_{1j}$ is the relative velocity between the two structures, where the jth device is located; u_{yj} is a displacement parameter; $\bar{A}_j = A_j u_{yj}$, $\bar{\beta}_j = \beta_j u_{yj}$, $\bar{\gamma}_j = \gamma_j u_{yj}$ and n_j are parameters which model the shape of the hysteresis loops.

By assuming that $\bar{\beta}_j + \bar{\gamma}_j = 1$ and $\bar{A}_j = 1$, the parameters F_{yj} and u_{yj}, respectively, correspond to yield force and yield displacement (Fig. 2).

2.2. Solution of equations of motion

The seismic input is here modeled as a Gaussian white-noise stationary stochastic process, which is characterized by the power spectral density S_0. The white-noise process is chosen in the analysis for its simplicity; however, the procedure proposed to find the solution to the equation of motion holds for general inputs [9,10].

By using the stochastic linearization technique, as discussed in a previous work [9], the hysteretic constitutive relation (Eq. (3)) can be replaced by the following linearized equation:

$$\dot{z}_j + \bar{C}_{ej}\Delta\dot{y}_j + \bar{K}_{ej} z_j = 0, \tag{5}$$

where for $n_j = 1$:

$$\bar{C}_{ej} = \sqrt{\frac{2}{\pi}}\left[\bar{\beta}_j\sqrt{\mathsf{E}[z_j^2]} + \bar{\gamma}_j\frac{\mathsf{E}[\Delta\dot{y}_j z_j]}{\sqrt{\mathsf{E}[\Delta\dot{y}_j^2]}}\right] - \bar{A}_j, \tag{6}$$

and

$$\bar{K}_{ej} = \sqrt{\frac{2}{\pi}}\left[\bar{\gamma}_j\sqrt{\mathsf{E}[\Delta\dot{y}_j^2]} + \bar{\beta}_j\frac{\mathsf{E}[\Delta\dot{y}_j z_j]}{\sqrt{\mathsf{E}[z_j^2]}}\right], \tag{7}$$

where the terms $\sqrt{\mathsf{E}[z_j^2]}$ and $\sqrt{\mathsf{E}[\Delta\dot{y}_j^2]}$ are, respectively, the standard deviations of variables z_j and $\Delta\dot{y}_j$, while $\mathsf{E}[\Delta\dot{y}_j z_j]$ is the covariance of the mentioned variables. Different expressions for $\bar{C}_{ej}$ and $\bar{K}_{ej}$ for $n_j \neq 1$ are reported in [14].

It is possible to rewrite Eqs. (1), (2) and (5) in the state space by using the following formulation:

$$\begin{cases} \dot{\mathbf{X}}(t) = \mathbf{A}\mathbf{X}(t) + \mathbf{B}e(t), \\ \mathbf{X}_e(t) = \mathbf{C}\mathbf{X}(t) + \mathbf{D}e(t), \end{cases} \tag{8}$$

in which $\mathbf{X}(t)$ is the $N \times 1$ state space vector ($N = 2N_1 + 2N_2 + N_u$); $\mathbf{A}$ the $N \times N$ matrix; $\mathbf{B}$ the $N \times N_u$ allocation input matrix; $\mathbf{X}_e(t)$ the $N_e \times 1$ output vector which depends on the number, N_e, of the selected response quantities, $\mathbf{C}$ and $\mathbf{D}$ are, respectively, the $N_e \times N$ allocation matrix and the $N_e \times 1$ direct-transformation vector. The quantities are defined as follows, where "T" indicates the transpose:

$$\mathbf{X}(t) = \begin{bmatrix} \mathbf{Y}_1^{\mathrm{T}} & \mathbf{Y}_2^{\mathrm{T}} & \mathbf{z}^{\mathrm{T}} & \dot{\mathbf{Y}}_1^{\mathrm{T}} & \dot{\mathbf{Y}}_2^{\mathrm{T}} \end{bmatrix}^{\mathrm{T}}, \tag{9}$$

$$\mathbf{B} = \begin{bmatrix} \mathbf{0} & \mathbf{0} & \mathbf{0} & \boldsymbol{\tau}_1^{\mathrm{T}} & \boldsymbol{\tau}_2^{\mathrm{T}} \end{bmatrix}^{\mathrm{T}}, \tag{10}$$

$$e(t) = -\ddot{y}_g(t), \tag{11}$$

$$\mathbf{A} = \begin{bmatrix} \mathbf{0} & \mathbf{0} & \mathbf{0} & \mathbf{I}_1 & \mathbf{0} \\ \mathbf{0} & \mathbf{0} & \mathbf{0} & \mathbf{0} & \mathbf{I}_2 \\ \mathbf{0} & \mathbf{0} & -\mathbf{K}_e & \mathbf{C}_e^{(1)} & -\mathbf{C}_e^{(2)} \\ -\mathbf{M}_1^{-1}\mathbf{K}_1 & \mathbf{0} & \mathbf{M}_1^{-1}\mathbf{F}_y^{(1)} & -\mathbf{M}_1^{-1}\mathbf{C}_1 & \mathbf{0} \\ \mathbf{0} & -\mathbf{M}_2^{-1}\mathbf{K}_2 & -\mathbf{M}_2^{-1}\mathbf{F}_y^{(2)} & \mathbf{0} & -\mathbf{M}_2^{-1}\mathbf{C}_2 \end{bmatrix}, \tag{12}$$

where ($i = 1, 2$): $\mathbf{I}_i$ is the $N_i \times N_i$ identity matrix; $\mathbf{C}_e{}^{(i)}$ is an $N_u \times N_i$ matrix where the first $N_u \times N_u$ part is a diagonal matrix $\mathbf{C}_e$ containing $\bar{C}_{ej}$ terms and the other parts are zero elements; $\mathbf{F}_y{}^{(i)}$ is the $N_i \times N_u$ matrix containing elements F_{yj} and zeros; $\mathbf{K}_e$ is an $N_u \times N_u$ diagonal matrix containing K_{ej} terms.

Since the excitation is stationary, this problem can be solved through the Liapunov equation:

$$\mathbf{A}\mathbf{G}_{\mathbf{XX}} + \mathbf{G}_{\mathbf{XX}}\mathbf{A}^{\mathrm{T}} + 2\pi S_0 \mathbf{B}\mathbf{B}^{\mathrm{T}} = \mathbf{0}, \tag{13}$$

where $\mathbf{G}_{\mathbf{XX}}$ is the $N \times N$ covariance matrix of the state space vector [10]. Eq. (13) is nonlinear because $\mathbf{A}$ depends on the response statistics trough $\mathbf{C}_e$ and $\mathbf{K}_e$ matrices; for this reason an iterative procedure is necessary. Rewriting the symmetric covariance matrix $\mathbf{G}_{\mathbf{XX}}$ into the one-dimensional vector $\mathbf{G}$, the solution is obtained by solving Eq. (13) iteratively until the following quantity $||\mathbf{G}^{k+1} - \mathbf{G}^k||/||\mathbf{G}^k|| \to 0$.

It is worthwhile to specify that each parameter contained in Eq. (1) has been normalized by the quantity $\sqrt{S_0}$. In particular, the force parameter in Eq. (2) is normalized as

$$F^*_{yj} = F_{yj}/\sqrt{S_0}. \tag{14}$$

2.3. Optimal design of hysteretic dampers

The aim of this study is the optimal design of nonlinear hysteretic devices interconnecting two adjacent structures described by a 2-mdof system (Fig. 1).

In order to perform the optimal design of nonlinear dissipative control systems, different criteria may be followed [1,16]. Among the large number of design methodologies, the criterion used in this work refers to an energy-based approach. Such criterion is associated with the concept of optimal performance of the dissipative connection. This concept means that the connection performs at its best if it is capable of dissipating the maximum amount possible of the earthquake input energy.

The optimization procedure to select the optimal device consists of maximizing an objective function named Energy Dissipation Index (EDI), proposed in [16]. The index is defined as the ratio of the maximum value of the energy dissipated in the dissipation devices, to the corresponding maximum value of the energy input by the earthquake, both evaluated over time. Maximizing the EDI index leads to a satisfactory optimal design for a large class of applications of dissipative passive control [16]. The definition of EDI, rearranged in the statistical representation [9], for one device ($N_u = 1$), has the expression:

$$\mathrm{EDI} = \frac{\mathsf{E}[\Delta E_{du}]}{\mathsf{E}[\Delta E_I]} = \frac{-\dfrac{\bar{K}_e}{F^*_y \bar{C}_e}\mathsf{E}[u^2]\Delta t}{(\sum_k \mathsf{m}_k + \sum_l \mathsf{m}_l)\pi\Delta t}, \tag{15}$$

in which $\mathsf{E}[\Delta E_{du}]$ represents the expected value of the increment of the energy dissipated by all the hysteretic devices, and $\mathsf{E}[\Delta E_I]$ represents the expected value of the increment of the total input energy introduced to the system by the seismic event, both normalized by $\sqrt{S_0}$. By making the two energy increments explicit, $\mathsf{E}[u^2]$ represents the expected value of the square of the control force u, obtained from the covariance matrix of the output vector $\mathbf{X}_e$, m_k and m_l (with $k = 1,2,\ldots,N_1$ and $l = 1,2,\ldots,N_2$) are the modal masses associated, respectively, with the kth and lth mode, and Δt is the time increment. Details about how the energy increments have been obtained are reported in [9].

Through this optimization procedure, the optimal design of passive control systems based on energy dissipation can be carried out. According to this procedure, the design of hysteretic devices interconnecting mdof structures implies the solution of a large number, n_e, of equations ($n_e = 2N_1 + 2N_2 + N_u$, Eq. (8)); moreover, equations must be solved iteratively. Finally, the increment of the energy dissipated by all the hysteretic connections and the increment of the total input energy in the system must also be calculated. It seems clear that the application of this methodology can be computationally wasteful.

Consequently, the next section proposes a simple procedure leading to the optimal design of the PCs by means of a simplified structural model.

3. Reduced order model: generalized 2-sdof system

3.1. Brief review on optimal design for 2-sdof system

In a previous work by the authors [9], the optimal design of a horizontal hysteretic dissipative link connecting two adjacent structures represented as a 2-sdof system was studied and solved.

Equations of motion for such 2-sdof systems (Fig. 3) excited by a base acceleration $a_g(t)$ were:

$$\begin{cases} \ddot{y}_1 + 2\xi_1\omega_1\dot{y}_1 + \omega_1^2 y_1 = \bar{F}_y z - a_g(t). \\ \ddot{y}_2 + 2\xi_2\sqrt{\frac{\lambda}{\mu}}\omega_1\dot{y}_2 + \frac{\lambda}{\mu}\omega_1^2 y_2 = -\frac{\bar{F}_y}{\mu} z - a_g(t), \end{cases} \tag{16}$$

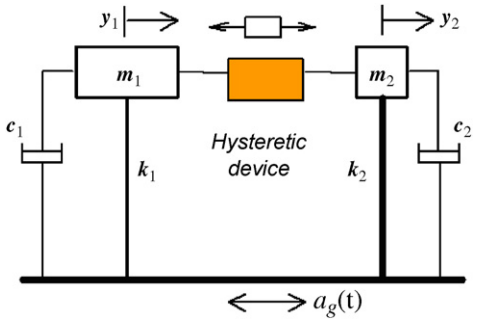

Fig. 3. The 2-sdof structural model.

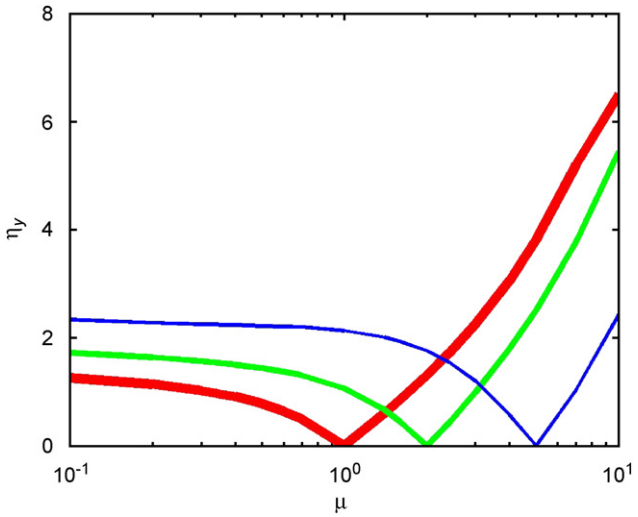

Fig. 4. Force design spectrum, $\lambda = 1$, $\lambda = 2$, $\lambda = 5$.

where ($i = 1, 2$): y_i is the relative displacement; ξ_i the damping ratio; ω_1 the natural frequency of the first structure; $\bar{F}_y = F_y/m_1$ the force in the PC normalized with respect to the mass m_1 of the first structure; λ and μ are, respectively, the stiffness ratio, $\lambda = k_2/k_1$, and the mass ratio, $\mu = m_2/m_1$; finally, z is described by the first-order Bouc–Wen equation, Eqs. (3) and (4), by assuming $j = 1$. The seismic input was modeled as a Gaussian white-noise stationary stochastic process, characterized by the power spectral density G_0.

In order to solve the nonlinear problem, the stochastic linearization technique explained in Section 2.2 was applied and z was represented by Eq. (5), always with $j = 1$. In this case, each parameter in Eq. (16) was normalized by the quantity $\sqrt{2G_0\omega_1}$. In particular, the force parameter was normalized as:

$$\eta_y = \bar{F}_y/\sqrt{2G_0\omega_1}. \tag{17}$$

The optimal device of the hysteretic connection was obtained by utilizing the energetic criterion explained in Section 2.3, Eq. (15).

The main results obtained in [9], performing a parametrical analysis for each couple of the structural parameters μ and λ were: (i) the optimal behavior of hysteretic device was found to be rigid plastic (the elastic stiffness of the connection $k_c = F_y/u_y \to \infty$); (ii) a synthetic optimal design spectrum for η_y had been obtained (Fig. 4); and (iii) the effectiveness of the connection on reducing vibrations has been demonstrated (Fig. 5).

In particular, by using Fig. 4, once the μ and λ values are known, it is possible to design the optimal hysteretic device by simply selecting the corresponding η_y parameter. The performance of the passive (optimal)

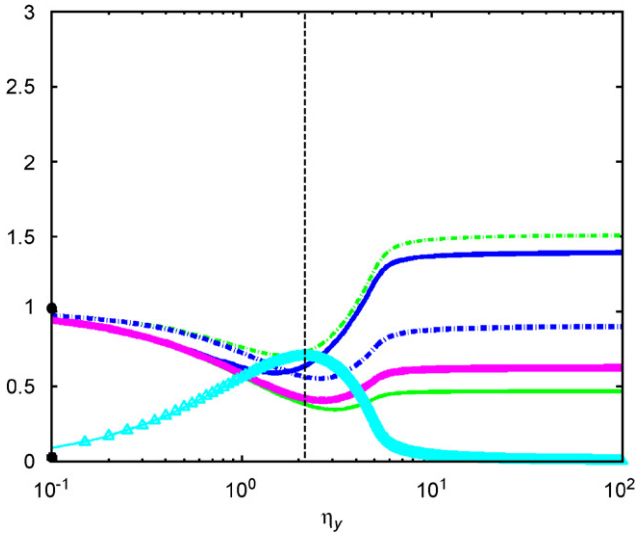

Fig. 5. EDI index and response quantities vs. η_y, $\mu = 1$, $\lambda = 5$. ● responses for $\eta_y = 0$. ■ EDI for $\eta_y = 0$. Y_1, Y_2, A_1, A_2, ΔY, EDI.

control is then evaluated in terms of response reduction. For example, for $\mu = 1$ and $\lambda = 5$, Fig. 5 shows the following response quantities vs. η_y: Y_i, A_i, $(i = 1, 2)$ and ΔY represent, respectively, the root mean square of the relative displacements, the absolute accelerations and the relative displacement between the structures, each normalized with respect to the case of no connection (NC). Moreover, the EDI index defined in Eq. (15) is also shown. The graph includes two limit situations: NC when $\eta_y \to 0$, and rigid connection when η_y reaches high values. Within these limit cases, the device works as a dissipative connection. It can be observed how the maximum EDI value selects the optimal parameter for the device ($\eta_y \cong 2.2$) and all the response quantities are significantly reduced, with respect to both limit cases.

The results discussed here may be applied to the optimal design of nonlinear hysteretic devices interconnecting 2-mdof adjacent structures. This objective is reached by utilizing a reduced order model, a generalized 2-sdof system, for the 2-mdof systems. The procedure will be explained in the following section.

3.2. Generalized 2-sdof system

It is worthwhile to study the 2-mdof system (Fig. 1), connected by hysteretic passive devices, by employing a generalized 2-sdof system, where each structure is represented by an elementary oscillator interconnected by a hysteretic device (Fig. 3).

In order to obtain a generalized 2-sdof system the principle of virtual displacement has been used [13]. By considering a model of 2-mdof structures interconnected by only one control device, $N_u = 1$, Eq. (1) may be rewritten in the form:

$$\begin{aligned} \mathbf{K}_1\mathbf{Y}_1(t) + \mathbf{C}_1\dot{\mathbf{Y}}_1(t) &= \mathbf{B}_{u1}^{\mathrm{T}}u(t) - \mathbf{M}_1\ddot{\mathbf{Y}}_1(t) - \mathbf{M}_1\boldsymbol{\tau}_1\ddot{y}_g(t), \\ \mathbf{K}_2\mathbf{Y}_2(t) + \mathbf{C}_2\dot{\mathbf{Y}}_2(t) &= -\mathbf{B}_{u2}^{\mathrm{T}}u(t) - \mathbf{M}_2\ddot{\mathbf{Y}}_2(t) - \mathbf{M}_2\boldsymbol{\tau}_2\ddot{y}_g(t). \end{aligned} \tag{18}$$

It is reasonable to consider only one device, as it has been demonstrated by numerical analysis that a small number of devices, one at least, is sufficient to obtain a good reduction of the seismic response. This result is already underlined in other works [10,12]. Moreover, as reminded by Section 3.1, and in order to simplify the explanation of the used procedure, a rigid plastic model described by the only yield force parameter F_y has been used for the device. In this case, Eq. (2) becomes:

$$u(t) = F_y z_r, \tag{19}$$

with

$$\dot{z}_r = [-\bar{\gamma}\,\mathrm{sgn}(\Delta\dot{y}_r)z_r|z_r|^{n-1} - \bar{\beta}|z_r|^n + \bar{A}]\Delta\dot{y}_r/u_y, \tag{20}$$

r being the rth degree of freedom where the device is placed.

In order to obtain the generalized 2-sdof system the displacements of the structures are approximately given as follows:

$$\mathbf{Y}_i(t) = \boldsymbol{\psi}_i q_i(t), \quad i = 1, 2, \tag{21}$$

where $\boldsymbol{\psi}_i$ are predefined vectors which give the displacement shapes along the structures, whereas $q_i(t)$ are the generalized displacements, depending on time. The shape function $\boldsymbol{\psi}_i$ must satisfy the displacement boundary conditions.

The principle states that if the equilibrate system is subject to virtual displacements $\delta\mathbf{Y}_i$, $(i = 1, 2)$ the external virtual work, δW_E, is equal to the internal virtual work, δW_I:

$$\delta W_E = \delta W_I. \tag{22}$$

By using Eq. (21), the increments of virtual displacements have the following expression:

$$\delta\mathbf{Y}_i = \boldsymbol{\psi}_i\,\delta q_i, \quad i = 1, 2. \tag{23}$$

By applying Eq. (22) and considering Eq. (18), (21), and (23) we obtain:

$$\begin{aligned}&\delta q_1\left[\boldsymbol{\psi}_1^{\mathrm{T}}\mathbf{M}_1\boldsymbol{\psi}_1\ddot{q}_1 + \boldsymbol{\psi}_1^{\mathrm{T}}\mathbf{C}_1\boldsymbol{\psi}_1\dot{q}_1 + \boldsymbol{\psi}_1^{\mathrm{T}}\mathbf{K}_1\boldsymbol{\psi}_1 q_1 - \boldsymbol{\psi}_1^{\mathrm{T}}\mathbf{B}_{u1}^{\mathrm{T}}F_y z_r + \boldsymbol{\psi}_1^{\mathrm{T}}\mathbf{M}_1\boldsymbol{\tau}_1\ddot{y}_g(t)\right]\\ &\quad + \delta q_2\left[\boldsymbol{\psi}_2^{\mathrm{T}}\mathbf{M}_2\boldsymbol{\psi}_2\ddot{q}_2 + \boldsymbol{\psi}_2^{\mathrm{T}}\mathbf{C}_2\boldsymbol{\psi}_2\dot{q}_2 + \boldsymbol{\psi}_2^{\mathrm{T}}\mathbf{K}_2\boldsymbol{\psi}_2 q_2 + \boldsymbol{\psi}_2^{\mathrm{T}}\mathbf{B}_{u2}^{\mathrm{T}}F_y z_r + \boldsymbol{\psi}_2^{\mathrm{T}}\mathbf{M}_2\boldsymbol{\tau}_2\ddot{y}_g(t)\right] = 0.\end{aligned} \tag{24}$$

Eq. (24) is satisfied when the two quantities within brackets are identically equal to zero for every virtual displacement $\delta q_i \neq 0$. Developing and rearranging Eq. (24), the following system of equations is obtained:

$$\begin{cases} m_1\ddot{q}_1 + c_1\dot{q}_1 + k_1 q_1 = \psi_{1r}F_y z_r - p_1\ddot{y}_g(t), \\ m_2\ddot{q}_2 + c_2\dot{q}_2 + k_2 q_2 = -\psi_{2r}F_y z_r - p_2\ddot{y}_g(t), \end{cases} \tag{25}$$

where $(i = 1, 2)$

$$\begin{aligned} &m_i = \boldsymbol{\psi}_i^{\mathrm{T}}\mathbf{M}_i\boldsymbol{\psi}_i, \quad c_i = \boldsymbol{\psi}_i^{\mathrm{T}}\mathbf{C}_i\boldsymbol{\psi}_i, \quad k_i = \boldsymbol{\psi}_i^{\mathrm{T}}\mathbf{K}_i\boldsymbol{\psi}_i,\\ &\psi_{ir} = \boldsymbol{\psi}_i^{\mathrm{T}}\mathbf{B}_{ui}^{\mathrm{T}}, \quad p_i = \boldsymbol{\psi}_i^{\mathrm{T}}\mathbf{M}_i\boldsymbol{\tau}_i. \end{aligned} \tag{26}$$

By assuming, $q_1 = \psi_{2r}y_1$ and $q_2 = \psi_{1r}y_2$, with $\psi_{1r}^2 = (p_2/p_1)(m_1/m_2)$ and $\psi_{2r}^2 = (p_1/p_2)(m_2/m_1)$, Eq. (25) is rewritten as:

$$\begin{cases} \ddot{y}_1 + \dfrac{c_1}{m_1}\dot{y}_1 + \dfrac{k_1}{m_1}y_1 = \dfrac{p_2F_y}{p_1m_2}z_r - \alpha\ddot{y}_g(t), \\ \ddot{y}_2 + \dfrac{c_2}{m_2}\dot{y}_2 + \dfrac{k_2}{m_2}y_2 = -\dfrac{p_1F_y}{p_2m_1}z_r - \alpha\ddot{y}_g(t), \end{cases} \tag{27}$$

where $\alpha = \sqrt{(p_1p_2)/m_1m_2}$; note that in Eq. (20) the relative velocity $\Delta\dot{y}_r$ at the rth degree of freedom is expressed as

$$\Delta\dot{y}_r = \mathbf{B}_{u2}\dot{\mathbf{Y}}_2 - \mathbf{B}_{u1}\dot{\mathbf{Y}}_1 = \psi_{2r}\dot{q}_2 - \psi_{1r}\dot{q}_1 = \psi_{1r}\psi_{2r}(\dot{y}_2 - \dot{y}_1) = \dot{y}_2 - \dot{y}_1 = \Delta\dot{y}. \tag{28}$$

Eq. (27) represents the expected generalized 2-sdof system. In fact, by comparing these equations and Eq. (16), the parameters of a generalized system may be identified and evaluated by using expressions shown in Table 1. Such equations are also formally equivalent, Eq. (28), for the parameters z_r, Eq. (20), and z. This means that it is possible to design the nonlinear hysteretic connection of 2-mdof adjacent structures by defining a generalized equivalent 2-sdof system, with dynamic features shown in Table 1, and by using the optimal design procedure discussed in Section 3.1, as will be explained below.

Table 1
Reduced order model parameters

Generalized 2-sdof system	2-sdof system
$\frac{k_1}{m_1}$	ω_1^2
$\frac{c_1}{m_1}$	$2\xi_1\omega_1$
$\frac{p_2 F_y}{p_1 m_2}$	$\bar{F}_y$
z_r	z
$\alpha\ddot{y}_g = \sqrt{\frac{p_1 p_2}{m_1 m_2}}\ddot{y}_g$	a_g
$\frac{k_2}{m_2}$	$\frac{\lambda}{\mu}\omega_1^2$
$\frac{c_2}{m_2}$	$2\xi_2\sqrt{\frac{\lambda}{\mu}}\omega_1$
$\left(\frac{p_2}{p_1}\right)^2\frac{m_1}{m_2}$	μ
$\frac{k_2}{k_1}\left(\frac{p_2 m_1}{p_1 m_2}\right)^2$	λ

3.3. Optimal design of hysteretic damper

The key step of the procedure is the evaluation of all parameters of generalized 2-sdof system through Table 1, such that, by taking into account Eq. (17), it is possible to evaluate the optimal force value for the device interconnecting 2-mdof adjacent structures, being $G_0 = \alpha^2 S_0$ and by using the spectrum of Fig. 4, in the following way:

$$F_y = \frac{p_1}{\psi_{1r}}\sqrt{2S_0\omega_1}\eta_y. \tag{29}$$

Finally, taking into account Eq. (14), the normalized optimal force is computed as

$$F_y^* = \frac{F_y}{\sqrt{S_0}} = \frac{p_1\sqrt{2\omega_1}}{\psi_{1r}}\eta_y. \tag{30}$$

4. Illustrative examples

In order to verify the developed methodology, three different numerical examples are considered. In the following, a detailed description of these cases is reported:

Case A: Two 10-story structures ($N_1 = N_2 = 10$) interconnected at their roof level by one hysteretic damper ($N_u = 1$ and $r = 10$). The mass of each floor for the structure "1" is 1.6×10^6 kg, for the structure "2" is 0.8×10^6 kg; the interstory stiffness for first structure is 0.6×10^{10} N/m, for the second structure it is 1.2×10^{10} N/m; finally, for both structures each mode has a damping ratio of 2%.

Case B: A flexible 20-story structure ($N_1 = 20$) interconnected to the roof of a stiff ten-story structure ($N_2 = 10$) by one hysteretic damper ($N_u = 1$, $r = 10$) [10]. For both the structures the mass of each floor is 1.6×10^6 kg, the interstory stiffness is 1.2×10^{10} N/m, and each mode has a damping ratio of 2%.

Case C: A four-story structure ($N_1 = 4$) interconnected to the roof of a stiff two-story structure ($N_2 = 2$) by one hysteretic damper ($N_u = 1$, $r = 2$). The mass of each floor for both structures is 125 kg, the stiffness matrices for structures 1 and 2 are:

$$\mathbf{K}_1 = 10^6 \times \begin{bmatrix} 7.23 & -3.53 & 0.22 & 0.16 \\ -3.53 & 6.12 & -3.45 & 0.15 \\ 0.22 & -3.45 & 6.9 & -3.5 \\ 0.16 & 0.15 & -3.5 & 3.13 \end{bmatrix} [\text{N/m}], \quad \mathbf{K}_2 = 10^6 \times \begin{bmatrix} 8.09 & -3.82 \\ -3.82 & 3.42 \end{bmatrix} [\text{N/m}],$$

the modal damping ratios of structures 1 and 2 are, respectively, $\xi_1 = 6.46, 2.21, 1.61, 1.75$, and $\xi_2 = 1.23, 0.8$. Such values are used to obtain the damping matrices $\mathbf{C}_1$ and $\mathbf{C}_2$. This example refers to a physical model used in an experimental campaign [17].

In all the applications hysteresis model parameters for the connecting dampers are taken as $\bar{A} = 1$, $\bar{\beta} = 0.5$, $\bar{\gamma} = 0.5$, and $n = 1$.

In order to investigate the influence of the shape of displacement vectors on the design problem, Eq. (21), three different $\boldsymbol{\psi}_i$, $(i = 1, 2)$, are chosen: (i) the first represents the first modal shape for each structure in a no-coupled case (NC); (ii) the second represents the first modal shape for each structure in a rigidly-coupled case (RC); (iii) in the last shape vector displacements have been assumed to increase linearly with the height above the base (linear deflection LD).

Note that in this work the optimal place of the device is not investigated. In all cases considered here, the device is always installed at the top of the low structure, $r = N_2$, as suggested in Refs. [10,12].

Two objectives must be reached for such examples:

(i) The primary objective is the optimal design of the hysteretic device performed by applying the developed method based on the reduced order model (see Section 3). In order to validate the proposed method, the results obtained with this procedure will be compared with the ones obtained by performing the optimal design on the 2-mdof adjacent structures (see Section 2.3). By summarizing the proposed procedure in few steps, the problem for each case is formulated in the following way:
   - to define the shape vectors $\boldsymbol{\psi}_i$, $(i = 1, 2)$;
   - to estimate the parameters of generalized 2-sdof system (Table 1);
   - to choose the optimal parameter η_y (Fig. 4);
   - to estimate the optimal force F_y* for 2-mdof system, Eq. (30).

(ii) The second objective is the evaluation of the effectiveness of hysteretic connection on the seismic response. Concerning this aspect, the response analysis is performed on the 2-mdof system. It is interesting to compare the responses of the passive controlled structures by means of the hysteretic connection, PC, with the situation of no-coupled structures, NC, and the situation of rigidly-coupled structures, RC, as already done with reference to the 2-sdof system, (see Section 3.1, Fig. 5).

The response quantities chosen for comparison are the root mean square of the relative displacement, the shear of the two structures, and the relative displacement between the two structures. It must be taken into account that each quantity has been normalized with respect to $\sqrt{S_0}$.

4.1. Case A: 10-10 mdof systems

This first example has been chosen because it refers to two structures which have equivalent degrees of freedom and the same floor elevation. In order to perform the optimal design of the hysteretic connection, the parameters in the generalized 2-sdof system are evaluated by using Table 1; some reduced order model parameters, computated for the assumed three shapes of the displacement vectors, are reported in Table 2.

By using Fig. 4 and with these values, it is possible to design the optimal force of hysteretic device F_y*, interconnecting the two structures, Eq. (30), for the three different shape vectors previously defined, see Fig. 6; these values are reported in Table 3.

Concerning the issue of choosing different shape displacement vectors, it appears that the structural parameters of the generalized 2-sdof system do not significantly change—see Table 2; in fact, the values of equivalent mass and stiffness ratios are similar. As a consequence, the force parameter η_y is equal; even ω_1, and the ratio p_1/ψ_{1r} parameters are quite similar, thus the optimal force F_y* selected with the simplified methodology is similar. Whatever shape vector is assumed, the optimal force selected has the same order of magnitude—see Table 3.

In order to validate the simplified methodology, the general procedure for the optimal design of a hysteretic connection in the 2-mdof system (introduced in Section 2), is also applied. For the two ten-story structures the EDI index has been calculated and the parametric analysis performed in order to get the best value of F_y* is carried out; the results are plotted in Fig. 7. The optimization leads to the optimal force value of

Table 2
Case A: 10-10 mdof system, reduced order model parameters

Ψ_i	λ	μ	η_y	ω_1	P_1/ψ_{1r}
NC	2	0.5	1.61	9.15	122.77×10^5
RC	1.98	0.49	1.61	9.76	140.40×10^5
LD	2	0.5	1.61	9.86	886×10^4

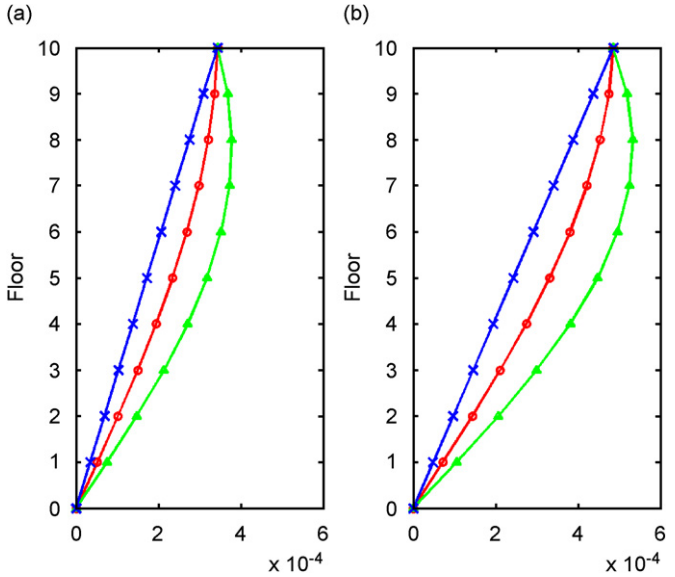

Fig. 6. Different shape vectors. NC: no-coupled case, RC: rigidly-coupled case, LD: linear deflection, for (a) structure 1, (b) structure 2.

Table 3
Case A: 10-10 mdof system, optimal parameter for different shape vectors

Ψ	F^*_y (N S$^{-3/2}$/m)
NC	7.4×10^7
RC	9.3×10^7
LD	6.3×10^7

$F_y^* = 7.5 \times 10^7$ [N s$^{-3/2}$/m], that is quite similar to those obtained with the simplified method. This demonstrates the validity of the simplified methodology proposed here. Furthermore, it appears that the choice of the shape vector does not substantially modify the result in terms of optimal force.

At this point, it is useful to investigate how the control device, designed here, leads to the reduction of the structural responses of the system. Figs. 8 and 9 show the displacement responses for the two structures. It can be noted that for both structures, the case of PC always reduces the responses if compared with the case of NC. In particular, for structure 1, the reduction of the top displacement with respect to NC is approximately equal to 70%, while for structure 2 the reduction is almost equal to 50%. It is also interesting to point out how the two rigidly connected structures behave. For structure 1, this link could guarantee a reduction of around 40% with respect to the case of NC, while for structure 2 an amplification of the response of approximately 42% is observed. In addition, better displacement reduction (for both structures) is obtained with the PC, rather than with the rigid connection. Fig. 10 shows the relative displacement between the structures. The case of PC results useful if compared with the case of NC; infact the roof reduction is around 70%. The rigid

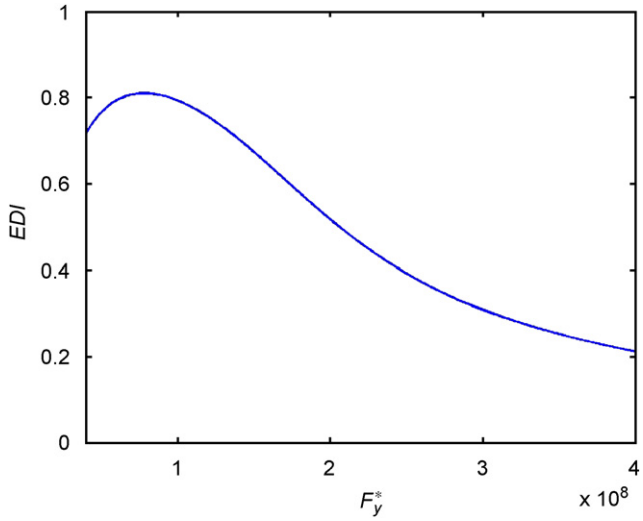

Fig. 7. Case A: 10-10 dof system, EDI index vs. F_y*.

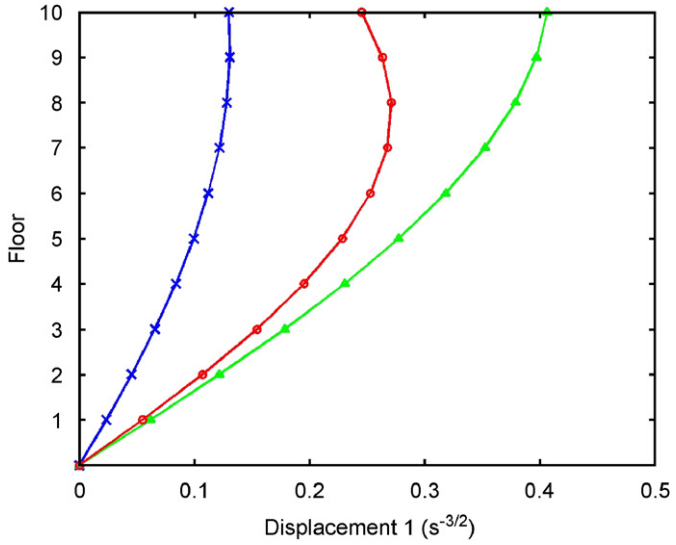

Fig. 8. Case A: 10-10 dof system, first structure displacement PC, NC, RC.

connection clearly acts in a manner which avoids the relative displacement at the roof level, but at lower levels the response can also increase if compared with the situation of PC. However, both ways of interconnecting the structures appear to be convenient for the reduction of relative displacement—of course this result was predictable on its own.

Finally, Fig. 11(a) and (b) shows the shear forces of the two structures. For structure 1, the situation with PC guarantees good reduction, both in comparison with the case of uncoupled structures than in rigidly coupled structure cases. In particular, the reduction of the base shear with respect to NC case is almost equal to 60%. Even for structure 2, good results are obtained by using the PC; the base shear appears reduced by around 60% in comparison with results obtained for uncoupled structures. Concerning shear force reduction by using the rigid connection, results are not as effective as for the passive case. In fact, structure 1 shows a response reduction with reference to NC especially at the lower floors (base shear reduction of around 45%), but in correspondence of the floor where the link is placed, an amplification is observed. Additionally, for structure 2 an amplification of the shear along all the elevation is also observed.

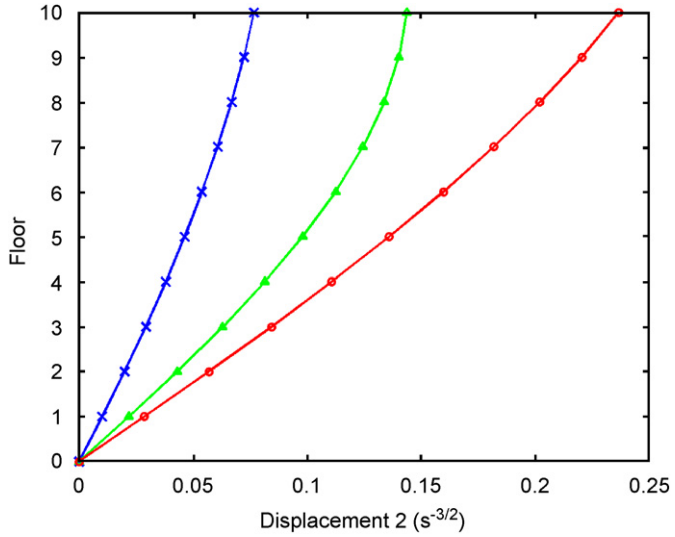

Fig. 9. Case A: 10-10 dof system, second structure displacement PC, NC, RC.

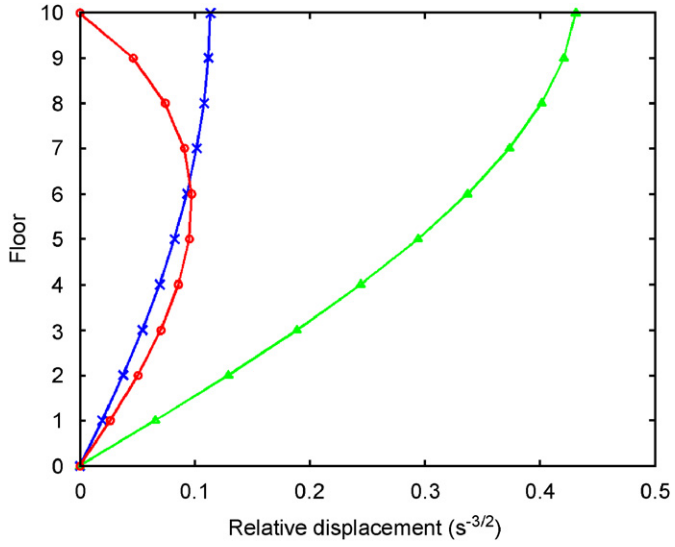

Fig. 10. Case A: 10-10 dof system, relative displacement between the structures PC, NC, RC.

Taking into account the objectives to be reached throughout the applications, it is possible to summarize for case A that:

(i) the simplified methodology is successful having conducted to the optimal force F_y* value in good accordance with the general procedure. Concerning the choice of shape displacement vectors ψ_i, it has been verified that optimal force F_y* has low dependence on the assumed shape. This circumstance has also been confirmed in the other examples and for this reason, in the following, only the results obtained with linear deflection will be shown;

(ii) a good performance in terms of response reduction has been obtained through the PC, since an effective suppression of the motion for the two structures has been observed, in comparison with both uncoupled and rigidly coupled structures.

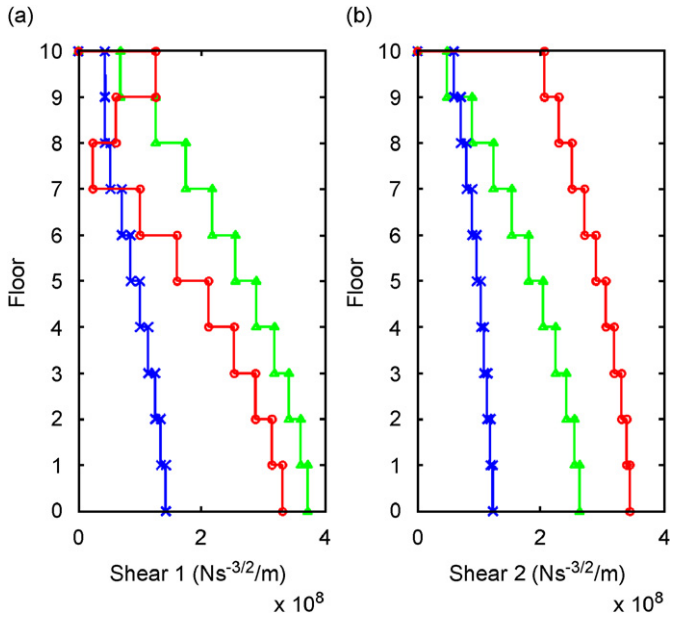

Fig. 11. Case A: 10-10 dof system, shear PC, NC, RC for (a) structure 1, (b) structure 2.

Table 4
Case B: 20-10 mdof system, reduced order model parameters

λ	μ	η_y	ω_1	P_1/ψ_{1r}
0.97	0.26	1.13	7.22	495.8×10^5

4.2. Case B: 20-10 mdof systems

This second case has been studied because the two structures do not have identical numbers of degrees of freedom. The aim is to demonstrate the validity of the simplified methodology in such situations, keeping in mind that this case is representative of typical structures in several engineering fields.

Some parameters in the generalized 2-sdof system are evaluated by means of the expressions shown in Table 1, and are summarized in Table 4. By using Eq. (30) the optimal force parameter obtained with the reduced order model is $F_y^* = 1.4 \times 10^8\,[\mathrm{N\,s^{-3/2}/m}]$.

Fig. 12 shows EDI index vs. F_y^*, in the 20 ten-story structures; the maximum value of EDI is attained for the optimal force value of $F_y^* = 1.3 \times 10^8\,[\mathrm{N\,s^{-3/2}/m}]$. Again, the simplified methodology and the general procedure match well in selecting the optimal force value F_y^*.

Figs. 13 and 14 show the displacement responses for the structures. As in the previous application, the case of PC, always reduces displacements along the elevation if compared with the case of NC. The top displacements of structures 1 and 2 are, respectively, reduced by approximately 50% and 60%, with respect to the case of NC. As for case A, the rigid connection, if compared with NC, improves the response of structure 1, but it has a negative effect on protection of structure 2. As a consequence, better displacement reduction (for both structures) is still obtained with the PC rather than with the rigid connection. Fig. 15 shows the relative displacement between the structures. With the PC, the relative displacement reduction at the roof with respect to the case of NC is more than 60%. For the particular characteristics of the two structures, (identical floor mass and interstory stiffness) relative displacement is avoided with the rigid connection.

Fig. 16(a) and (b) shows the shear force of the two structures. On the elevation a good reduction is reached through the hysteretic link, having the base of around 50% of reduction for both structures with respect to the

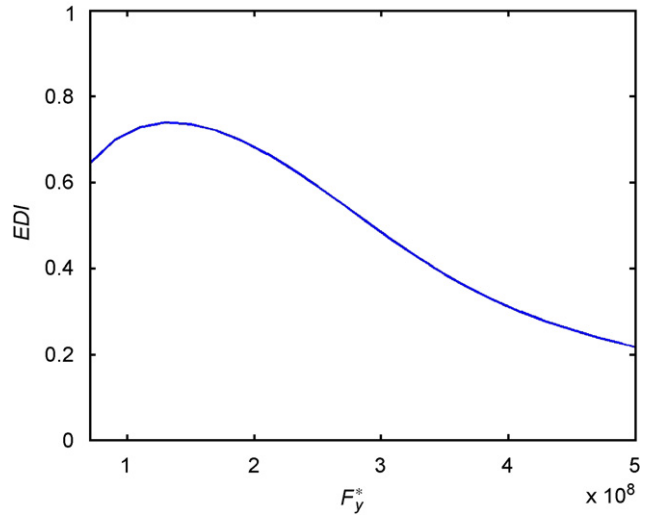

Fig. 12. Case B: 20-10 dof system, EDI index vs. F_y*.

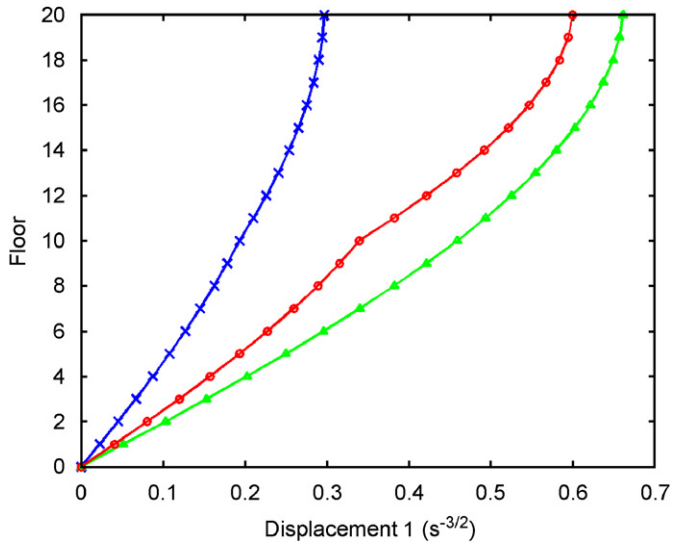

Fig. 13. Case B: 20-10 dof system, first structure displacement PC, NC, RC.

case of NC. The solution obtained with a rigid connection compared with respect to case NC, contrarily, furnishes reduction only for structure 1 and only for the first nine floors. From the 10th floor, where the link is supposed to act, a large jump is noticed. Even observing the shear force on the elevation for the PC case, a little increase at the 10th floor appears; however, the response preserves reduction in the upper floors. Structure 2 shows large amplification in the RC case. Interconnecting with a rigid device does not appear to be a convenient solution for such adjacent structures. Even in case B, the effectiveness of PC is demonstrated and appears to be a good solution for response reduction among the different connections proposed here.

4.3. Case C: 4-2 mdof systems

The third case deals with the physical model of two actual structures subject to dynamic tests on a shaking table [17] (Fig. 17). Such structures are interconnected with a hysteretic steel-yielding device, designed for the

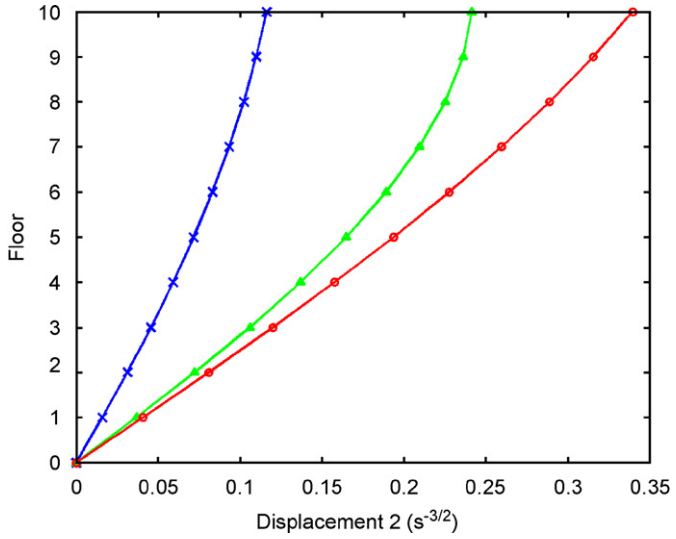

Fig. 14. Case B: 20-10 dof system, second structure displacement PC, NC, RC.

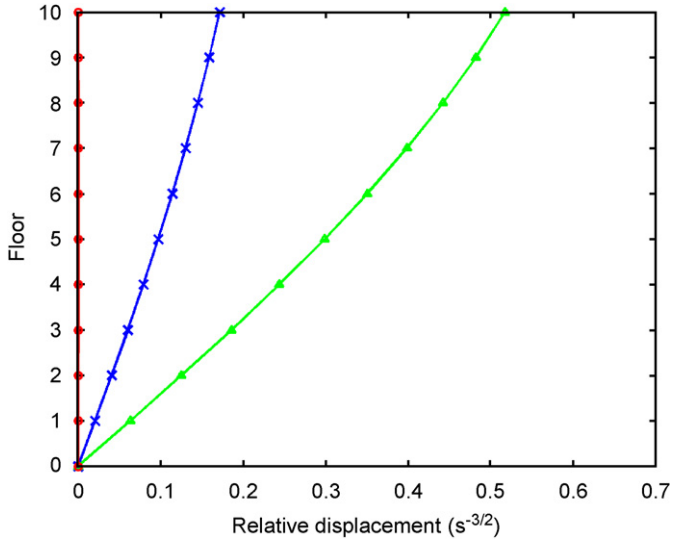

Fig. 15. Case B: 20-10 dof system, relative displacement between the structures PC, NC, RC.

experimental campaign by using the discussed method presented here. Even this example involves the response of two structures having different degrees of freedom. As done for the previous examples, the structural parameters, in the generalized 2-sdof system, are reported in Table 5.

The optimal force obtained with the reduced order model using Eq. (30) is $F_y^* = 6937\,[\mathrm{N\,s^{-3/2}/m}]$. By performing the optimal design on the 2-mdof system, the maximization of the EDI index vs. F_y^* leads to the value $F_y^* = 6500\,[\mathrm{N\,s^{-3/2}/m}]$, as shown in Fig. 18. Again the two methodologies yield quite similar results.

Figs. 19 and 20 show the displacement responses of the structures. For the particular characteristics of this system, both solutions (PC and RC) of interconnecting the adjacent structures imply a reduction for the displacements, if compared with the case of NC. In any case, the PC is better than the rigid connection. In fact, with respect to the NC situation, the reduction of the top displacement for structure 1 is almost 30% for the PC case, whereas the reduction is less than 10% for the RC case. For structure 2, reductions of approximately 60% for the PC case and 30% for RC case, are observed. Fig. 21 shows the relative displacement between the

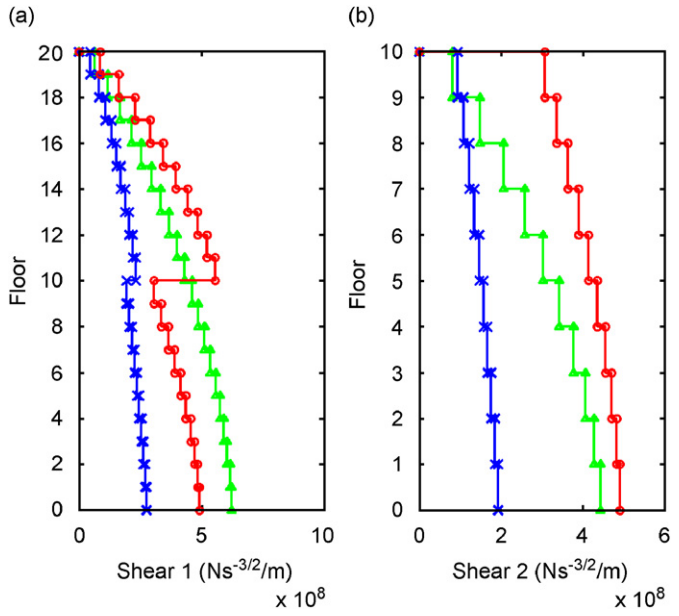

Fig. 16. Case B: 20-10 dof system, shear PC, NC, RC for (a) structure 1, (b) structure 2.

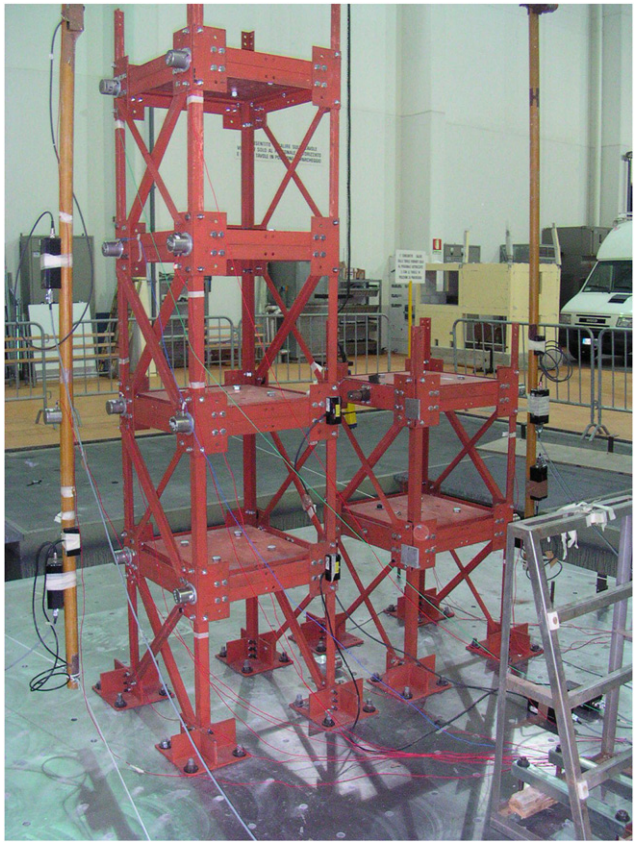

Fig. 17. Physical model of the 4-2 dof structures.

Table 5
Case C: 4-2 mdof system, reduced order model parameters

λ	μ	η_y	ω_1	P_1/ψ_{1r}
1.24	0.3	1.11	49.96	637.81

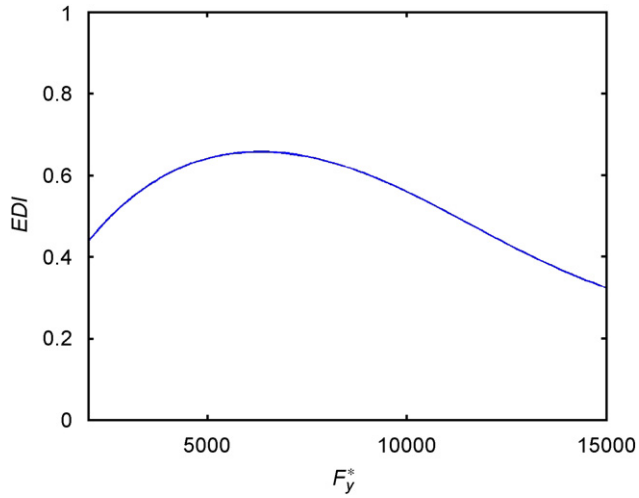

Fig. 18. Case C: 4-2 dof system, EDI index vs. F_y*.

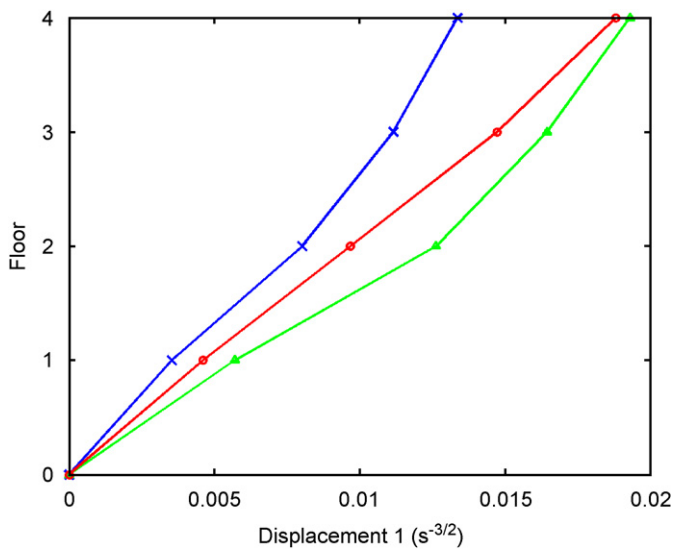

Fig. 19. Case C: 4-2 dof system, first structure displacement PC, NC, RC.

structures. Also in this case a reduction of almost 60% of the response is observed by interconnecting structures with the passive device, with respect to NC. In this case, the reduction obtained with a rigid connection is greater than that obtained with a PC. Fig. 22(a) and (b) shows the shear force of the two structures. The PC guarantees good and regular reductions of the shear force on the elevation for both structures. The reduction at the base is around 30% for structure 1, and around 40% for structure 2. A rigid link shows improvements in terms of displacements for structure 2 with respect to the case for NC, but, for

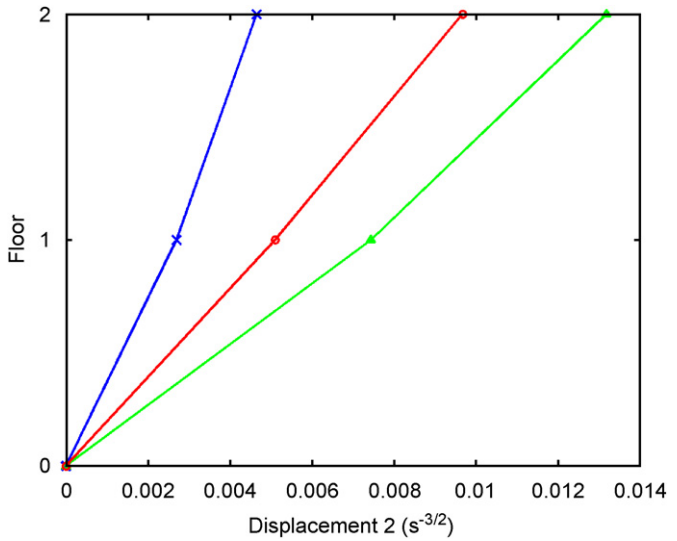

Fig. 20. Case C: 4-2 dof system, second structure displacement PC, NC, RC.

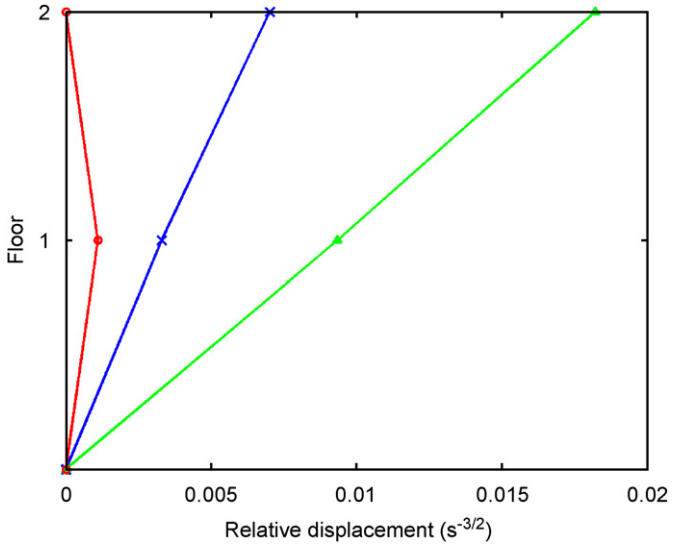

Fig. 21. Case C: 4-2 dof system, relative displacement between the structures PC, NC, RC.

structure 1, an amplification of the shear force is shown with a large jump at the last floors. In any case, the best performance is obtained by using the hysteretic device.

In this example, the best advantages due to the presence of the interconnection are observed regarding structure 2. In fact, all the response quantities attain the largest reduction.

5. Conclusions

A reduced order model for optimal design of 2-mdof structures, connected by hysteretic dampers, has been studied. The seismic input has been modeled as a Gaussian white-noise stationary stochastic process, whereas the passive nonlinear hysteretic connection has been modeled by the differential Bouc–Wen law. In order to simplify the problem, a stochastic linearization technique has been applied. The design procedure is based on replacing a 2-mdof system, with a generalized 2-sdof system, in which each structure is represented by an

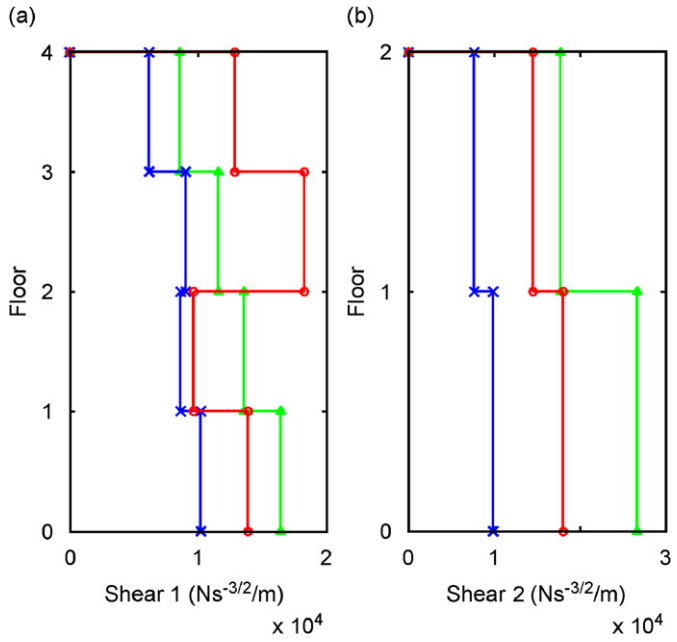

Fig. 22. Case C: 4-2 dof system, shear PC, NC, RC for (a) structure 1, (b) structure 2.

elementary oscillator interconnected by a hysteretic device. Assuming predefined vectors which give the displacement shape along the structures, it has been possible to obtain the expected reduced order model by applying the principle of virtual displacements. Once the equivalent structural parameters of the generalized 2-sdof system have been discovered, the optimal design of the connection is carried out by using simple spectra obtained by the authors in a previous work, where the optimal design of a horizontal hysteretic link connecting 2-sdof systems has been studied and solved.

Illustrative examples have been treated in order to reach double objectives:

(i) performing the optimal design of the hysteretic device by applying the developed method based on the reduced order model. In order to validate the proposed method, the results obtained with this procedure have been compared with the results obtained by performing the optimal design on the 2-mdof adjacent structures by using the energetic criterion;
(ii) the evaluation of the effectiveness of hysteretic connection on the seismic response by performing the response analysis on the 2-mdof system.

Results confirm the proposed methodology as successful for the optimal design of the connection. Concerning the choice of shape displacement vectors, it has been verified that optimal force parameter has low dependence on the assumed shape; for this reason a linear deflection has been selected for the analysis. Moreover, the PC led to good performances in terms of response reductions; this is directly due to an effective suppression of the motion for the two structures, in comparison with both no-coupled and rigidly-coupled structures, which have been observed.

References

[1] G.W. Housner, L.A. Bergman, T.K. Caughey, A.G. Chassiakos, R.O. Claus, S.F. Masri, R.E. Skelton, T.T. Soong, B.F. Spencer, J.T.P. Jao, Structural control: past, present and future, *Journal of Engineering Mechanics* 123 (9) (1997) 897–971.
[2] T.T. Soong, B.F. Spencer Jr., Supplemental energy dissipation: state-of-the-art and state-of-the-practice, *Journal of Engineering Structures* 24 (2002) 243–259.

[3] Y.K. Wen, Method for random vibration of hysteretic systems, *Journal of the Engineering Mechanics Division, Proceedings of the American Society of Civil Engineers* 102 (1976) 249–263.
[4] H.P. Zhu, Y.L. Xu, Optimum parameters of Maxwell model-defined dampers used to link adjacent structures, *Journal of Sound and Vibration* 279 (2005) 253–274.
[5] H.P. Zhu, H. Iemura, A study of response control on the passive coupling element between parallel structures, *Structural Engineering and Mechanics* 9 (4) (2000) 383–396.
[6] Y.L. Xu, Q. He, J.M. Ko, Dynamic response of damper-connected adjacent buildings under earthquake excitation, *Engineering Structures* 21 (1999) 135–148.
[7] T. Aida, T. Aso, K. Takeshita, T. Takiuchi, T. Fujii, Improvement of the structure damping performance by interconnection, *Journal of Sound and Vibration* 242 (2) (2001) 333–353.
[8] A. Filiatrault, B. Folz, Nonlinear earthquake response of structurally interconnected buildings, *Canadian Journal of Civil Engineering* 18 (4) (1992) 560–572.
[9] M. Basili, M. De Angelis, Optimal passive control of adjacent structures interconnected by non-linear hysteretic devices, *Journal of Sound and Vibration* 301 (2007) 106–125.
[10] Y.Q. Ni, J.M. Ko, Z.G. Ying, Random seismic response analysis of adjacent buildings coupled with non-linear hysteretic dampers, *Journal of Sound and Vibration* 246 (2001) 403–417.
[11] Z.G. Ying, Y.Q. Ni, J.M. Ko, Non-linear stochastic optimal control for coupled-structures system of multi-degree-of-freedom, *Journal of Sound and Vibration* 274 (2004) 843–861.
[12] A.V. Bhaskararao, R.S. Jangid, Seismic analysis of structures connected with friction dampers, *Engineering Structures* 28 (5) (2006) 690–703.
[13] A.K. Chopra, *Dynamics of Structures: Theory and Applications to Earthquake Engineering*, Prentice Hall, Englewood Cliifs, NJ, 2001.
[14] Y.K. Wen, Equivalent linearization for hysteretic systems under random excitation, *ASME Journal of Applied Mechanics* 47 (1980) 150–154.
[16] V. Ciampi, M. De Angelis, Optimal design of passive control systems based on energy dissipation for earthquake protection of structures, *Proceedings of the Third European Conference on Structural Dynamics, EURODYN*, Firenze, Italia, 1996.
[17] G. Cimellaro, M. De Angelis, E. Renzi, V. Ciampi, Theory and experimentation on passive control of adjacent structures, *13th World Conference on Earthquake Engineering*, Vancouver, BC, Canada, 2004.

Further reading

[15] A. Filiatrault, S. Cherry, Seismic design spectra for friction damped structures, *Journal of Structural Engineering ASCE* 116 (5) (1990) 1334–1355.